Heavy Quark Production at HERA

Andreas B. Meyer

University of Hamburg

1 Introduction

Heavy quark production in ep scattering predominantly occurs via the process of boson gluon fusion (BGF, see fig.1a,e). The cross section is thus directly sensitive to the gluon distribution in the proton. In photoproduction the photon virtualities are small ($Q^2 \sim 0$), and the photon can reveal a hadronic structure. In a leading order picture, the production process can be divided into direct photon (fig.1a) or resolved photon (fig.1b-e) processes. In the latter the photon acts as a source of incoming quarks and gluons, and only a fraction of the photon momentum participates in the hard scattering.

In the kinematic region $p_T^2 \leq m_{c,b}^2$ it is expected that next–to leading order (NLO, $O(\alpha_S^2)$) QCD calculations in the so-called massive scheme will give reliable results. In this scheme u, d and s are the only active quark flavours in the proton and heavy quarks are dynamically produced via BGF. In contrast, in the massless scheme, valid for $p_T^2 \geq m_{c,b}^2$, the heavy quarks are treated as sea quarks in the proton and in the resolved photon. Single charm (or beauty) quarks can then directly emerge from within the photon (fig.1b-d).

Quantitative theoretical predictions of observable heavy quark event properties and cross sections are obtained from pQCD. The fragmentation functions are generally taken from previous e^+e^- experiments assuming universality. The measurement of heavy flavour processes at the HERA ep collider is then a powerful means of exploring the dynamics of perturbative QCD

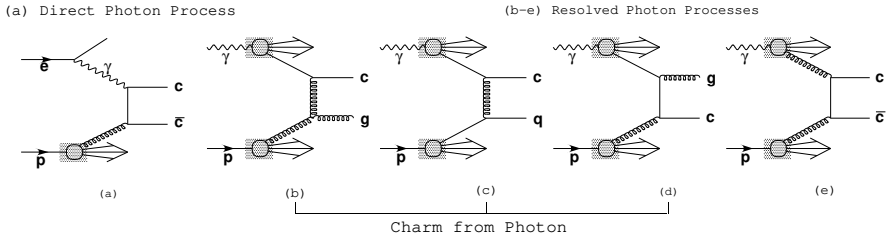

Fig. 1. Processes of direct and resolved heavy quark production. At $Q^2 > 1$ GeV^2 the contribution from resolved photon processes is small.

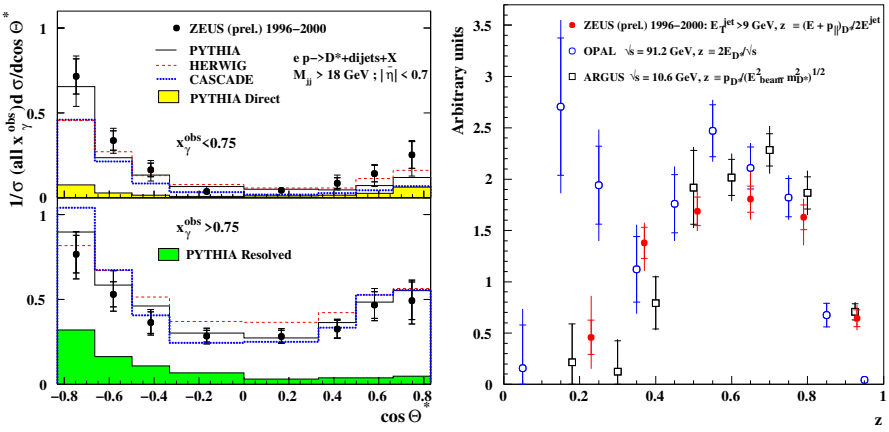

Fig. 2. a) Relative differential cross sections $1/\sigma d\sigma/d\cos\theta^*$ in two regions of $x_\gamma^{\rm obs}$. The shaded area for $x_\gamma^{\rm obs} > 0.75$ ($x_\gamma^{\rm obs} > 0.75$) is the contamination of the direct (resolved) photon contribution. b) fragmentation measurement as a function of $z = (E + p_L)_D/(E + p_L)_{\rm jet}$ for the ZEUS data [4] and $z = E_D/E_{\rm beam}$ for the e^+e^- experiments OPAL and ARGUS.

and testing the universality assumptions for the parton distributions and fragmentation models.

In the following, recent experimental results obtained at the HERA ep collider are reviewed in both photoproduction and electroproduction (DIS: $Q^2 \geq 1$ GeV^2) at a ep center of mass energy $\sqrt{s} = 320$ GeV.

2 Open Charm Production

New results on inclusive D-Meson production are available from H1 [1] and ZEUS [2]. The D-Mesons are identified in the detectors by reconstruction of the relevant decay chains $D^{*+} \to D^0\pi^+$, $D^0 \to K^-\pi^+$ or $D^0 \to K^-\pi^+\pi^-\pi^+$, $D_s \to \phi\pi$ and $D^+ \to K^-\pi^+\pi^+$ in the visible kinematic regions of transverse momentum $p_t(D)$ and pseudorapidity $\eta(D)$. For the H1 measurements the charm lifetime properties are exploited using a two layer silicon vertex detector to obtain results in the DIS region. Comparisons of the D-Meson measurements with theoretical predictions show that the data are generally well described [1] by the LO Monte Carlo generator AROMA. The ZEUS results show that in photoproduction the NLO theory tends to be lower than the data in particular at large values of p_T and η [2].

In order to probe the details of the charm production dynamics and to study the contribution from charm quarks emerging from the photon the angular distributions of charmed di-jet events are studied by the ZEUS experiment in photoproduction (fig.2a) [3]. To distinguish experimentally between direct and resolved photoproduction the variable $x_\gamma^{\rm obs}$ is used which describes

the momentum fraction of the parton emerging from the photon in the proton rest system: $x_\gamma^{\rm obs} = (\sum_{\rm jet1,2} E_T e^{-\eta^{\rm jet}})/(2yE_e)$ where yE_e corresponds to the energy of the incoming photon in the proton rest system. For direct photon gluon fusion $x_\gamma \sim 1$ while for resolved photoproduction $x_\gamma^{\rm obs}$ is smaller. A cut at $x_\gamma^{\rm obs} = 0.75$ is used to separate the two processes. The normalised cross section $1/\sigma\ d\sigma/d(\cos\theta^*)$ is shown in fig.2a as a function of the angle of the incoming proton and the jet associated with the D^* meson in the photon proton center of mass system. In the region of $x_\gamma^{\rm obs} < 0.75$ (upper histogram) the resolved component is enriched and for $x_\gamma > 0.75$ (lower histogram) the direct component dominates. For positive (negative) values of $\cos\theta^*$ the D^* is produced in the direction of the incoming proton (photon). The cross section for the region of $x_\gamma < 0.75$ is asymmetric in $\cos\theta^*$ rising sharply towards large negative $\cos\theta^*$ values which indicates sizable contributions from boson propagators and hence that there is a sizable fraction of events with the charm quark emerging from within the photon (processes fig.1b,c).

The question of the universality of non-perturbative fragmentation effects has been addressed by both H1 and ZEUS. The energy fraction $z = (E+p_L)_D/(E+p_L)_{\rm jet}$ as measured by ZEUS [4] is shown in fig.2b. Within the framework of the LO simulation (in Pythia) and a Peterson fragmentation parametrization an optimal fragmentation parameter $\epsilon_{Pete} = 0.064 \pm 0.006^{+0.011}_{-0.008}$ has been extracted. The H1 results on inclusive production of D-mesons in DIS for the vector D^{*+} and the peudoscalar mesons D^0, D_s and D^+ [1] have been used to extract the fragmentation ratios of the different D-meson quark and spin states and to compare them with the numbers obtained at e^+e^- colliders. The results have comparable precision to those from LEP and support the assumption of fragmentation universality.

3 Charmonium

In a fraction of events, the charm quarks form a bound charmonium state and both inelastic J/ψ and $\psi(2S)$ production have been measured [5,6]. In calculations the process is treated within the framework of non–relativistic QCD (NRQCD) where the cross section is a sum over all possible intermediate $c\bar{c}$ states, including colour singlet (CS) and colour octet (CO) states. The amplitude for each $c\bar{c}$ state with definite colour and angular momentum factorises into a short distance term which can be calculated and a long distance matrix element (LDME) describing the transition to a J/ψ. The LDMEs are not calculable, but should be the same in all processes. They have been determined from J/ψ production data in $p\bar{p}$ collisions [7] where the CO contributions were found to be sizable.

Figure 3 shows the H1 and ZEUS photoproduction data [6]. Good agreement is seen. The data are well described by a NLO calculation [8] in the Colour Singlet Model. In contrast, the LO calculation falls more steeply in $p^2_{t,\psi}$. The elasticity distribution (fig.4a) can also be described by LO NRQCD

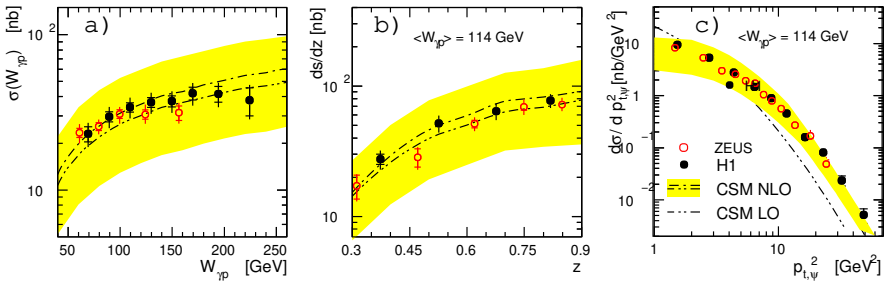

Fig. 3. a) Inelastic J/ψ photoproduction cross section as a function of $W_{\gamma p}$ and differential cross sections as functions of b) $p^2_{t,\psi}$ and c) z. The ZEUS points [6] are shifted by up to 12% to account for differences in the covered kinematic range. The CSM calculations in NLO is shown by the band. The normalization uncertainties are due to variations of α_s and the charm mass m_c.

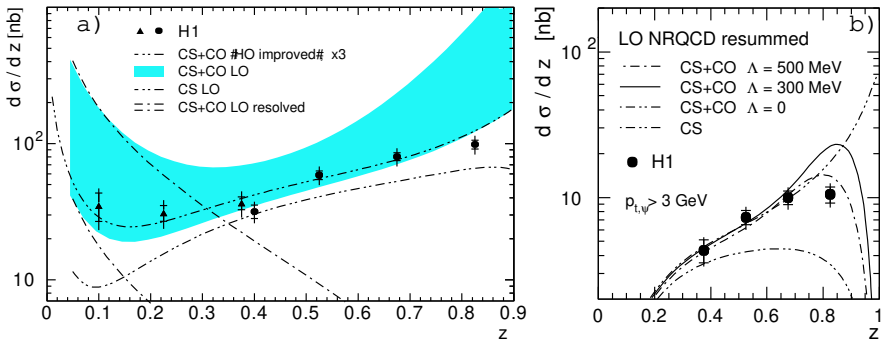

Fig. 4. Differential J/ψ photoproduction cross section as a function of z a) in comparison to NRQCD calculations [9]; b) for $p_{t,\psi} > 3\,\mathrm{GeV}$ in comparison with a resummed NRQCD calculation [10] (scaled by a factor 3). The parameter Λ describes the energy loss of the J/ψ due to soft gluon emission

calculations [9] with LDMEs for the colour octet contributions at the lower end of the range allowed by the Tevatron data. The steeper rise of the NRQCD calculations towards high z than that in the data may be due to phase space limitations for the emission of soft gluons in the transition from the $c\bar{c}$ state to the J/ψ meson which are not considered in this calculation [9]. A resummation [10] of the non–relativistic expansion, which is valid at large $p_{t,\psi}$, leads to a slowing of the increase and better agreement with the data (fig.4b).

4 Beauty Production

Previous measurements of open beauty production at HERA relied on the transverse momentum p_t^{rel} of the muon produced in the semi-leptonic decay

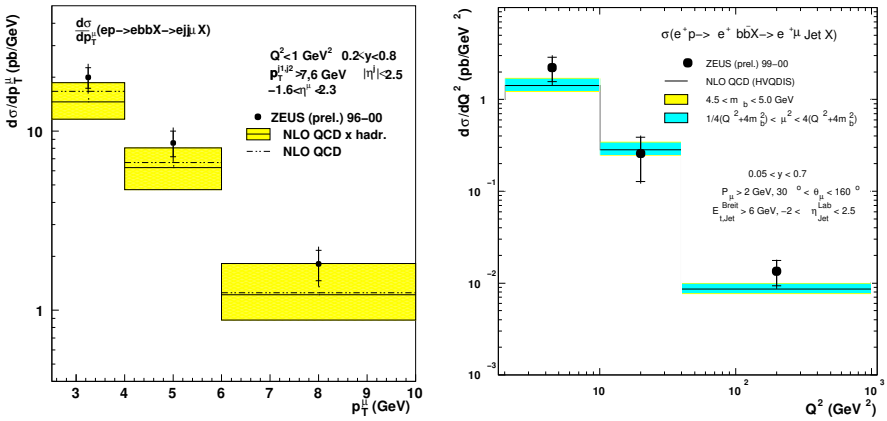

Fig. 5. Differential beauty cross sections as measured by ZEUS compared with NLO QCD calculations a) in photoproduction ($Q^2 \sim 0$) as a function of p_t^μ [12,14] and b) in DIS as a function of Q^2 [13,16]

with respect to the axis of the closest jet and also by exploiting the b-lifetime using Si-Detectors [11]. New differential cross sections using the $p_t^{\rm rel}$-method for events with two jets and a muon in the final state [12,13] are now available from ZEUS. Fig.5a shows the measured photoproduction cross section differential in p_T^μ in the kinematic region $Q^2 < 1$ GeV^2, $0.2 < y < 0.8$, $p_T^{jet_{1(2)}} > 7(6)$ GeV, $|\eta^{jet_{1(2)}}| < 2.5$, $p_T^\mu > 2.5$ GeV and $-1.6 < \eta^\mu < 2.3$ in comparison with a NLO QCD calculation (FMNR) [14]. For the predictions, the hadronisation is modeled by a Peterson function and the spectrum of the semi-leptonic muon momentum was extracted from PYTHIA [15]. The band shows the results obtained by variation of the b-quark mass, the renormalization and the factorization scales. The measured cross sections are a factor of 1.4 larger than the central NLO prediction but compatible with it within the experimental and systematic uncertainties. Using PYTHIA to extrapolate to the unmeasured part of the muon kinematics and to correct for the branching ratio, the total cross section for dijet production in $b\bar{b}$ events $\sigma(ep \to b\bar{b}X \to jjX)$ has been determined to be $733 \pm 61 \pm 104$ pb while the NLO QCD prediction is 381^{+117}_{-78} pb, corresponding to a data excess of a factor of two. The $p_t^{\rm rel}$ method has also been applied to DIS events at $Q^2 > 2$ GeV^2 with at least one muon in the final state and at least one jet. A total visible cross section of $\sigma^{\rm vis} = 38.7 \pm 7.7^{+6.1}_{-5.0}$ pb was measured for the reaction $ep \to eb\bar{b}X \to ej\mu X$ in the kinematic region $0.05 < y < 0.7$, $p^\mu > 2$ GeV, $30^\circ < \theta^\mu < 160^\circ$ with one jet in the Breit frame of $E_T^{\rm Breit} > 6$ GeV and $-2 < \eta^{\rm Lab} < 2.5$. In fig.5b the differential cross section $d\sigma/dQ^2$ is compared with a NLO QCD calculation as implemented in the HVQDIS program [16]. The NLO prediction is $28.1^{+5.3}_{-3.5}$ pb which agrees with the measured value within the errors.

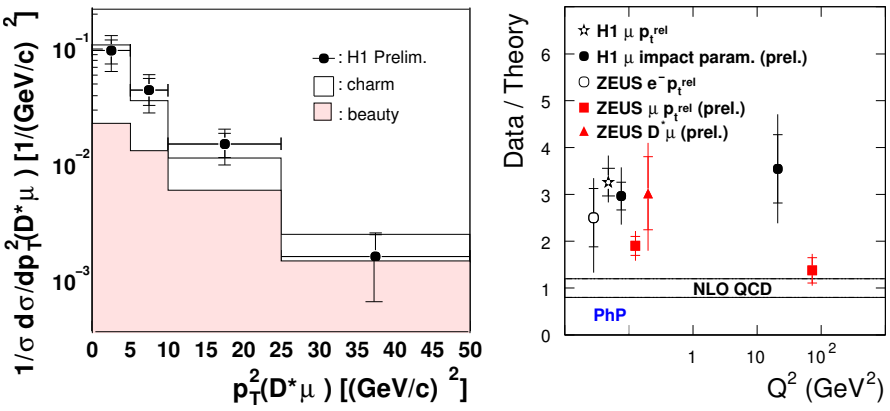

Fig. 6. a) Normalised visible $D^*\mu$ cross section differential in $p_t^2(D^*\mu)$. The simulated charm contribution is shown by the shaded histogram. b) Summary of the results on b-production obtained at HERA so far [11–13].

The charm and beauty contributions to double heavy flavour tagged samples can also be separated by exploiting the charge and angle correlations of a D^* meson and a muon produced in the reaction $ep \to eb\bar{b}X$. The configuration in which the muon and the D^* originate from the same parent B-meson yielding unlike sign $D^*\mu$ pairs measured in the same hemisphere is of particular interest. H1 has extracted the cross sections of beauty and charm production using a likelihood fit in the region $p_T^{D^*} > 1.5$ GeV, $|\eta| < 1.5$, $p_T^\mu > 1$ GeV, $|\eta^\mu| < 1.74$ and $0.05 < y < 0.75$ [17] (fig.6a). The measured b-cross section is $\sigma_{\rm vis}^b = 380 \pm 120 \pm 130$ pb, about a factor of 3.8 larger than the LO Monte Carlo expectation. ZEUS have conducted a similar analysis [18] in a slightly different phase space, $p_T^{D^*} > 1.9$ GeV, $|\eta| < 1.5$, $p_T^\mu > 1.4$ GeV, $-1.75 < \eta^\mu < 1.3$ yielding a cross section $\sigma_{\rm vis}^b = 214 \pm 52^{+96}_{-84}$ pb. The H1 and ZEUS results agree when the same cuts are applied. The ZEUS results are compared with NLO QCD predictions in the region $Q^2 < 1$ GeV^2, $0.05 < y < 0.85$ and in the b-quark rapidity range $\eta^b < 1$ where the distributions of the Monte Carlo program agree with the respective FMNR spectra. The extrapolated cross section is $\sigma(\gamma p \to b(\bar{b})X) = 15.1 \pm 3.9^{+3.8}_{-4.7}$ nb while the NLO prediction of FMNR for this reaction is only $5.0^{+1.7}_{-1.1}$ nb.

5 Summary

New results on heavy quark production at HERA have been presented.

In the D-meson data general agreement with the theoretical expectations is found. Dijet angular distributions indicate a strong contribution to the resolved photoproduction cross section from charm quarks in the photon. The results on fragmentation support the universality assumption.

The results on inelastic charmonium photoproduction are well described by NLO calculations with colour singlet contributions alone and thus exhibit no indication for colour octet contributions.

A precise quantitative understanding of the b-quark production mechanism is still an open question. The HERA results obtained so far are summarised in fig.6b. A set of new visible cross sections of beauty production, defined without extrapolation beyond the detector acceptance have been measured. The results are a factor 1.4 higher than the NLO QCD predictions but consistent within the experimental and theoretical uncertainties. Data and theory are also consistent in the DIS regime. An excess of the measured cross sections over the NLO expectation is observed when the data is extrapolated into kinematic regions not directly measured.

The HERA collider is now starting a new phase of operation at higher luminosities. Together with the enhanced c and b-tagging capabilities of the new H1 and ZEUS vertex detectors more precise and differential measurements can be expected within the next years.

References

1. H1 collab., contr.paper 1015 to ICHEP 2002, Amsterdam.
2. ZEUS collab., contr.paper 786 to ICHEP 2002, Amsterdam.
3. ZEUS collab., contr.paper 781 to ICHEP 2002, Amsterdam.
4. ZEUS collab., contr.paper 778 to ICHEP 2002, Amsterdam.
5. C. Adloff *et al.* [H1 Coll.], Eur. Phys. J. C**25** (2002) 1, 25-39.;
   C. Adloff *et al.* [H1 Coll.], Eur. Phys. J. C**25** (2002) 1, 41-53.
6. S. Chekanov *et al.* [ZEUS Collaboration], arXiv:hep-ex/0211011.
7. F. Abe *et al.* [CDF Coll.], Phys. Rev. Lett. **79** (1997) 572.
8. M. Krämer, Prog. Part. Nucl. Phys. **47** (2001) 141. ;
   B.A. Kniehl and G. Kramer, Eur. Phys. J. C **6** (1999) 493.
9. M. Krämer, Nucl. Phys. B**459** (1996) 3.
10. M. Beneke, G.A. Schuler and S. Wolf, Phys. Rev. D **62** (2000) 034004.
11. H1 Coll., C.Adloff et al, Phys.Lett. B 467, 156 (1999);
    ZEUS Coll., J.Breitweg et al., Eur.Phys.J. C**18**, 625 (2001);
    H1 Coll., contr.paper 1013 to ICHEP 2002, Amsterdam.
12. ZEUS Coll., contr.paper 785 to ICHEP 2002, Amsterdam.
13. ZEUS Coll., contr.paper 783 to ICHEP 2002, Amsterdam.
14. M. Cacciari, S.Frixione and P.Nason, JHEP 0103, 006 (2001).
15. E.Norrbin and T.Sjostrand, Eur. Phys. J. C**17** (2000) 137.
16. B.W.Harris and J.Smith, Phys. Rev. D**57** (1998) 2806.
17. H1 Coll., contr.paper 1016 to ICHEP 2002, Amsterdam.
18. ZEUS Coll., contr.paper 784 to ICHEP 2002, Amsterdam.